CREO
CENTRO RICERCHE ELETTRO OTTICHE

HIPER-OSR
-
EXECUTIVE SUMMARY REPORT

ISSUE	Date	Change Records	Author	Distribution List
01	22/06/2022	1st emission	S. Mengali (CREO)	CREO, UNISOTON, ESTEC

TABLE of CONTENTS

List of acronyms and abbreviations

α	Solar absorptance
Al	Alluminum
Al_2O_3	Allumina (Alluminum Oxide)
Δε	Emissivity contrast ($\Delta\varepsilon = \varepsilon_{hot} - \varepsilon_{cold}$)
ε	Infrared emittance
ε_{cold}	Infrared emittance at low temperature
ε_{hot}	Infrared emittance at high temperature
BoL	Begin of Life
EBL	Electron Beam Lithography
EoL	End of Life
IR	Infrared Radiation
LESR	Low Emissivity Solar Reflector
MgF_2	Magnesium Flouride
OSR	Optical Solar Reflector
PMA	Perfect Metamaterial Absorber
QWOT	Quarter Wavelength Optical Thickness
SiO_2	Silica (Silicon Dioxide)
T_{MIT}	Metal-to-Insulator transition Temperature
TO	Thermo-Optical
UV	Ultra-Violet radiation
VIS	Visible radiation
VO_2	Vanadium Dioxide
W	Tungsten
YF_3	Yttrium Fluoride

1. Project objectives

The high-level objective of HIPER-OSR was to develop a new class of Optical Solar Reflectors (OSR) characterized by being *smart* and *flexible*, whereas:

- Smart means that emittance varies with temperature, from low emittance in the cold state (solar flux low or absent / system in sleep or safe mode) to high emittance in the hot state (solar flux high, system fully operational);
- Flexible means that the proposed OSR consists of a meta-material coating deposited on an Aluminum film.

The proposed coating architecture is shown in Figure 1:

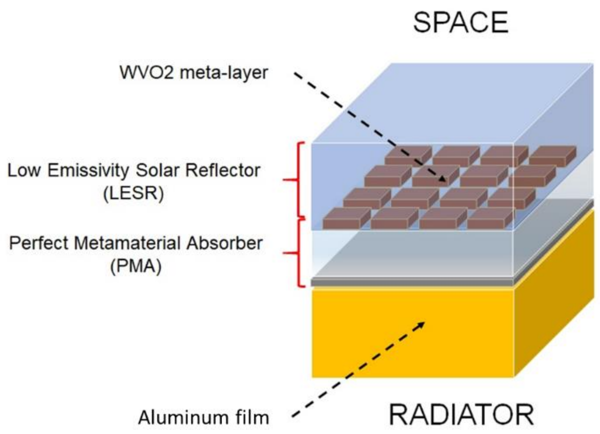

Figure 1: Coating architecture.

In brief, the coating is made of two functional blocks, that is a temperature-variable emitter and a Low Emittance Solar Reflector:

- The variable emitter is a Perfect Metamaterial Absorber PMA, that is it consists of a metal back-reflector, a dielectric spacer, and an array of micron-size squares of thermochromic VO2. At high temperature, the VO2 islands are in the metal phase and interact with the back-reflector generating high emittance. At low temperature, VO2 islands change into a dielectric phase and interactions with the metal back-reflector are switched off → emittance is substantially reduced. The operating principle is similar to a classical Fabry-Perot configuration: in the latter the pattern is replaced by a continuous layer of VO2. The main advantage of the metamaterial configuration is reduced solar absorptance α due to the reduced fill factor of VO2 (which is highly absorptive across the entire visible spectrum).
- The solar reflector is added to reduce solar absorptance further. It consists of the superposition of several dielectric filters all made of materials that are transparent both in the VIS and in the thermal IR spectrum. IR transparency is here necessary to enable radiative coupling between the variable emitter and the outer space.

All the layers of the two blocks are deposited by sputtering, while the array is patterned by Electron Beam Lithography EBL.

2. Project structure

In order to achieve the project objectives, activities were organized in four work-packages as follows:

- WP1: Requirements
- WP2: Materials, multi-layers and breadboards
- WP3: Test samples
- WP4: Testing and technology validation

The work was carried out by CREO as main contractor and by the University of Southampton in charge of optical simulations and final optical design definition.

Activities started in September 2018 and ended in June 2022, with significant delays due in part to the COVID crisis, in part to technical challenges and to difficulties at booking test facilities.

3. Work done and achievements

Requirements

The requirements for the final technology demonstrators were defined in terms of performance and endurance as follows:

- Thermo-optical performance at the Begin of Life:
  - Solar Absorbance BoL $\alpha \leq 0.24$;
  - Hot state emittance $\varepsilon_{hot} \geq 0.8$;
  - Emittance contrast $\Delta\varepsilon = \varepsilon_{hot} - \varepsilon_{cold} > 0.4$;
  - Transition Temperature $T_{MIT} \approx 25°C$.

- Stable mechanical and thermo-optical properties after:
  - Thermovacuum cycles and thermal endurance tests;
  - Humidity tests;
  - (UV radiation test: low doses);
  - Proton radiation test at doses equivalent to 2 years in GEO orbit.

UV radiation test is placed in brackets because in the end it could not be performed due to project delays.

Materials, multi-layers and breadboards

Efforts were aimed primarily at developing 1) W-doped VO2 layers having phase transition at room temperature; 2) VO2 patterns compatible with the overall coating structure and fabrication workflow; 3) sputter-deposited high and low index materials transparent across the VIS and the IR spectrum; 4) preliminary design and breadboards suitable to verify the proposed technical solution:

- W-doped VO2 thermochromic layers: after initial unsuccesfull attempts we developed a two-step process in which W-doped VO2 is first deposited at room temperature by co-sputtering, then annealed in vacuum at 375°C for about 45'. The process is compatible with Kapton and Aluminum substrates and allows to control with good accuracy and reproducibility the position and strength of the transition at ≈ 25°C.

- VO2 patterns: we developed a multi-step process that starts with the definition of a photoresist pattern on the dielectric spacer by EBL, continues with the deposition and lift off of the VO2 pattern, and ends with the thermal vacuum treatment of the pattern at 375°C. The process is capable to produce the square patterns designed by UNISOTON with good accuracy and reproducibility.
- Materials for the solar reflector: after identifying ZnS and MgF2 as candidate materials for the LESR, we succeeded at developing a sputtering process for ZnS, but failed with MgF2: all attempts led to high absorbance in the VIS, or very poor adhesion, or too low deposition rates. Next, we replaced pure MgF2 with MgF2:SiO2 composites and found that the presence of SiO2 at about 50% volume ratios is effective at stabilizing the mechanical properties and at improving transparency in the VIS spectrum. This, however, is payed at the cost of reduced IR transparency due to the strong vibrational band of SiO2 at 9.5 µm wavelength.
- Design and breadboards: several designs were modelled, in which: a) the dielectric spacer is either SiO2 or ZnS; b) the VO2 meta-layer is made of squares and gaps of variable size at the µm scale; c) the LESR is made of a reduced number (< 20) of layers of ZnS and MgF2:SiO2. The most promising designs were translated into small breadboards on Silicon and Kapton. The main finding was that the LESR was still too thin to reduce α to acceptable values and yet thick enough to dampen appreciably the contrast generated by the variable emitter. Therefore, new efforts were made to find a better low index material for the LESR, having lower IR absorbance. We started by raising the MgF2 volume ratio in the MgF2:SiO2 composite, from 50% to 80%, with modest improvements. Next, we studied a different composite system, with YF3 in place of MgF2, to arrive at a final composition YF3:SiO2 = 30:70 having fair IR transparency and mechanical stability. The new low index material was used to design and build solar reflectors made of up to 3 filters and 29 layers. Fine tuning of the optical design was not possible because of the very long duration of the deposition process (more than one week)

Test samples

With the improved LESR now available, we proceeded to build a total of three test samples 30 mm x 30 mm on Aluminum film: the structure is in Table 1, images in Figure 2.

Table 1: structure of the test samples

Layer	Material	Thickness	Notes
Substrate	Polished Al	130 µm	
Adhesion	Al_2O_3	10-20 nm	
Back-reflector	Al	200-250 nm	
Dielectric spacer	SiO_2	900 nm	
TC pattern	W-doped VO_2	30 nm	Pattern geometry: - squares: 2700nm - gaps: 1000 nm
Adhesion layer	Al2O3	70-100 nm	
LESR	ZnS YF_3:SiO_2 = 30:70	1≈ 2µm	Multilayered QWOT stack. Superposition of 3 filters.
Cap layer	Al_2O_3	30 nm	

Figure 2: Test samples glued on Al2O3 plates for testing. Size: 30 x 30 mm^2; pattern: 10 x 10 mm^2.

Testing and technology validation

The three samples were tested according to the sequence shown in Figure 3. Thermo-optical properties and visual appearance were monitored during the sequence, adhesion was tested on one sample at the end of the sequence.

TO properties BoL and EoT are given in Table 2 and Table 3, respectively; adhesion test result is shown in Figure 4.

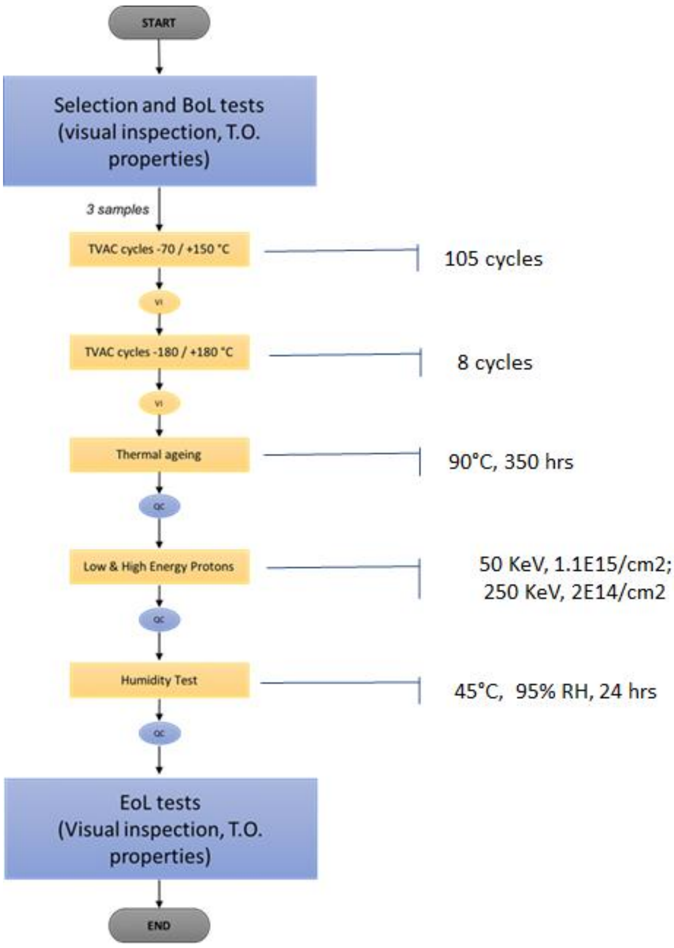

Figure 3: executed test sequence

Table 2: T.O. properties at BoL

Sample ID	α_{hot}	ε_{hot}	$\Delta\varepsilon$	T_{MIT} (°C)	ΔT_{MIT} (°C)
HO_Al_20201001#01	0.46±0.01	0.78±0.01	0.28±0.02	27±2	30±5
HO_Al_20201001#02	0.44±0.01	0.74±0.01	0.28±0.02	39±2	30±5
HO_Al_20201001#03	0.45±0.01	0.75±0.01	0.30±0.02	34±2	30±5

Table 3: T.O. properties at EoT. Variations from BoL in brackets, in red if meaningful.

Sample	α_{hot}	ε_{hot}	$\Delta\varepsilon$	T_{MIT} (°C)	ΔT_{MIT} (°C)
HO_Al_20201001#01	0.46±0.01 (--)	0.82±0.01 (+0.04)	0.22±0.02 (-0.06)	37±2 (+10)	30±5 (--)
HO_Al_20201001#02	0.42±0.01 (-0.02)	0.81±0.01 (+0.07)	0.19±0.02 (-0.09)	40±2 (+1)	30±5 (--)
HO_Al_20201001#03	0.43±0.01 (-0.02)	0.80±0.01 (+0.05)	0.23±0.02 (-0.07)	38±2 (+4)	30±5 (--)

Figure 4: Adhesion tape test at EoT

Results can be summarized as follows:

- Mechanical stability is good: no change of appearance is detected after the tests, and no coating fragment is observed on the tape after the adhesion test;
- α is high at BoL, and shows no variation after the tests;
- ε_{hot} is aligned with the target at BoL, and improves slightly after the tests;
- $\Delta\varepsilon$ is a bit weak at BoL, and becomes weaker after the tests. Deeper analysis shows that contrast degradation occurs in the first hot cycles of the TVAc test, and is probably due to chemical interaction between VO_2 and Al_2O_3. This suggests that Al_2O_3 should be replaced by other more inert material at the VO_2 interfaces.
- T_{MIT} is a bit high, but not far from the target.

4. Conclusions

Project results were not entirely satisfactory. In particular, great difficulties were encountered in the realization of the solar reflector by sputtering, which led to final coatings having high solar absorbance and relatively weak emittance contrast. Furthermore, the contrast was found to degrade after thermal cycling, probably due to chemical interactions at the interface between the thermochromic pattern and the contiguous layers.

At the same time, the technical failures of the project served us as a lesson and starting point for conceiving and exploring alternative configurations and growth methods. In particular, in the frame of the project 'Smart-Flex' that started after HIPER-OSR and was funded by the European Commission, we studied configurations that, although based on the same architecture of Figure 1, utilize a solar reflector made of pure ZnS and pure YF_3 deposited by electron-gun evaporation. This approach allowed us to achieve $\alpha < 0.24$, $\Delta\varepsilon > 0.30$, $T_{MIT} \approx 25°C$, and stable thermo-optical and mechanical properties after thermal vacuum cycling, humidity, and protons. Moreover, the results obtained in HIPER-OSR and Smart-Flex gave us new ideas and development directions to further improve the performance of the device and to fully satisfy the application requirements.

In conclusion, although HIPER-OSR was not a technical success in itself, it represents an important intermediate step in the development of a technology that has the potential to deliver in the near future a new class of Optical Solar Reflectors that are both smart and flexible.

– End of Document –